Supplementary Material

Live-cell quantitative monitoring reveals distinct, high-affinity Gβγ regulations of GIRK2 and GIRK1/2 channels.

Reem Handklo-Jamal[1], Tal Keren Raifman[1], Boris Shalomov[1], Patrick Hofer[3], Uri Kahanovitch[1], Theres Friesacher[3], Galit Tabak[1], Vladimir Tsemakhovich[1], Haritha P. Reddy[1, ¶], Orna Chomsky-Hecht[4], Debi Ranjan Tripathy[1,4], Kerstin Zuhlke[5], Carmen W. Dessauer[6], Enno Klussmann[5,7], Yoni Haitin[1,2], Joel A. Hirsch[2,4], Anna Stary-Weinzinger[3], Daniel Yakubovich[8], Nathan Dascal[1,2]

[1] Department of Physiology and Pharmacology, School of Medicine, Tel Aviv University, Tel Aviv, Israel
[2] Sagol School of Neuroscience, Tel Aviv University, Tel Aviv, Israel
[3] Department of Pharmaceutical Sciences, Division of Pharmacology and Toxicology, University of Vienna, Josef-Holaubek-Platz 2, 1090 Vienna, Austria.
[4] Department of Biochemistry & Molecular Biology; Institute of Structural Biology, George S. Weiss Faculty of Life Sciences, Tel Aviv University, Tel Aviv, Israel
[5] Max-Delbrück-Center for Molecular Medicine in the Helmholtz Association (MDC), Berlin, Germany
[6] Department of Integrative Biology and Pharmacology, University of Texas Health Science Center, Houston, Texas, USA
[7] DZHK (German Centre for Cardiovascular Research), partner site Berlin, Germany
[8] The Adelson School of Medicine, Ariel University, Ariel 4077625, Israel

[¶] Present address: Department of Neuroscience, Faculty of Health and Medical Sciences, University of Copenhagen, Blegdamsvej 3B, 2200 Copenhagen N, Denmark

Correspondence to: Nathan Dascal dascaln@tauex.tau.ac.il, Daniel Yakubovich danielya@ariel.ac.il

Supplementary Methods

Modeling GIRK1/2 basal activity and activation by expression of Gβγ with four kinetic models

To describe GIRK1/2 activation by Gβγ with the inclusion of a mechanistic explanation of I_{basal}, we utilized 4 gating models (Supplementary Fig. 8a): #1, concerted activation, non-cooperative binding; #2, concerted activation, cooperative binding; #3, graded contribution, non-cooperative binding; and #4, graded contribution, cooperative binding model. Concerted activation models are based on the assumption of four Gβγ required for channel opening. The concerted activation, cooperative binding model #2 is the modified WTM model used throughout this paper. Graded contribution models are based on increasing contribution to $P_{o,max}$ of each sequential Gβγ-bound state. We have previously described the graded contribution non-cooperative binding model[1], and the graded contribution cooperative binding model was described in detail by Berlin et al.[2].

Since the basal activity of GIRK12 is highly Gβγ-dependent, and this phenomenon was shown to be dependent on differential recruitment of Gα and Gβγ to the GIRK1/2 microenvironment[3], we first utilized each of the four models of Supplementary Fig. 8a to estimate the basal endogenous Gα and Gβγ available for channel's gating ($G\alpha_{endo}$ and $G\beta\gamma_{endo}$, where endo stays for endogenous).

For calculations we used the following parameters: $P_{o,max}$ (open probability value, observed with 5 ng Gβ RNA and 1-2 Gγ RNA) ~ 0.105[1], P_o in the absence of Gβγ ~0.00273 (assuming 10% Gβγ-independent activity out of total I_{basal} of GIRK1/2 , $P_{o,basal}$ = 0.0273 (open probability in absence of Gβγ expression, c=26 % of maximal open probability; Fig. 4F) and Po, agonist = 0.0525 (open probability corresponding to full endogenous Gβγ dissociation from Gα induced by agonist, which is 50% of that of $P_{o,max}$ with 5 ng Gβ RNA[1]. Utilizing the $P_{o,max}$ and single channel current, we estimated channel density to be 13.7 channels/μm^2. The above described data were substituted to system of equations relevant for each model as described[1, 2] and solved in Matlab 6.5 for Windows. This procedure was conducted for a range of K_d values, thus generating initial values matrix containing [K_d, $G\beta\gamma_{endo}$, $G\alpha_{endo}$]. Estimated values are shown in Supplementary Fig. 8b. Each [K_d, $G\beta\gamma_{endp}$, $G\alpha_{endo}$] was subsequently utilized for simulation of a complete dose response to expressed Gβγ. In order to make calculations more time-efficient, the dose response was simulated as a steady-state solution of a system of differential equations. Gating schemes described in Fig.S8a were combined with agonist-independent G-protein dissociation reaction:

(1) $$G\alpha_{GDP} + G\beta\gamma \underset{k_{off,G}}{\overset{k_{on,G}}{\rightleftarrows}} G\alpha_{GDP}G\beta\gamma$$

where $G\alpha_{endo}=G\alpha_{GDP}+G\alpha_{GDP}G\beta\gamma$ and $G\beta\gamma_{endo}=G\beta\gamma+G\alpha_{GDP}G\beta\gamma$, and $G\alpha_{endo}$ and $G\beta\gamma_{endo}$ are calculated values obtained for each K_d value as described above.

Simulation of models based on cooperative binding of Gβγ to the channel was based on solution of the following differential equations system:

(2) $dG\alpha_{GDP}/dt=k_{off,G}\cdot G\alpha_{GDP}G\beta\gamma-k_{on,G}\cdot G\alpha_{GDP}\cdot G\beta\gamma$

(3) $dG\beta\gamma/dt= k_{off,G}\cdot G\alpha_{GDP}G\beta\gamma+k_{off}\cdot(C_1+2\cdot\mu\cdot C_2+3\cdot\mu^2\cdot C_3+4\cdot\mu^3\cdot C_4)-$

$- G\beta\gamma\cdot(k_{on,G}\cdot G\alpha_{GDP}+4\cdot k_{on}\cdot C_0+3\cdot k_{on}\cdot C_1+2\cdot k_{on}\cdot C_2+ k_{on}\cdot C_3)$

(4) $dG\alpha_{GDP}G\beta\gamma/dt= k_{on,G}\cdot G\alpha_{GDP}\cdot G\beta\gamma- k_{off,G}\cdot G\alpha_{GDP}\cdot G\beta\gamma$

(5) $dC_0/dt= -4\cdot k_{on}\cdot G\beta\gamma\cdot C_0+k_{off}\cdot C_1$

(6) $dC_1/dt=4\cdot k_{on}\cdot G\beta\gamma\cdot C_0-3\cdot k_{on}\cdot G\beta\gamma\cdot C_1- k_{off}\cdot C_1+ 2\cdot\mu\cdot k_{off}\cdot C_2$

(7) $dC_2/dt=3\cdot k_{on}\cdot G\beta\gamma\cdot C_1-2\cdot k_{on}\cdot G\beta\gamma\cdot C_2- 2\cdot\mu\cdot k_{off}\cdot C_2+3\cdot\mu^2\cdot k_{off}\cdot C_3$

(8) $dC_3/dt=2\cdot k_{on}\cdot G\beta\gamma\cdot C_2-1\cdot k_{on}\cdot G\beta\gamma\cdot C_3- 3\cdot\mu^2\cdot k_{off}\cdot C_3+4\cdot\mu^3\cdot k_{off}\cdot C_4$

(9) $dC_4/dt=1\cdot k_{on}\cdot G\beta\gamma\cdot C_3- 4\cdot\mu^3\cdot k_{off}\cdot C_4$

Simulation for model based on non-cooperative binding of Gβγ to channel was based on solution of the following differential equations system:

(10) $dG\alpha_{GDP}/dt=k_{off,G}\cdot G\alpha_{GDP}G\beta\gamma-k_{on,G}\cdot G\alpha_{GDP}\cdot G\beta\gamma$

(11) $dG\beta\gamma/dt= k_{off,G}\cdot G\alpha_{GDP}G\beta\gamma +k_{off}\cdot(C_1+2\cdot\mu\cdot C_2+3\cdot\mu^2\cdot C_3+4\cdot\mu^3\cdot C_4)-$
$-G\beta\gamma\cdot(k_{on,G}\cdot G\alpha_{GDP}+4\cdot k_{on}\cdot C_0+3\cdot k_{on}\cdot C_1+2\cdot k_{on}\cdot C_2+ k_{on}\cdot C_3)$

(12) $dG\alpha_{GDP}G\beta\gamma/dt= k_{on,G}\cdot G\alpha_{GDP}G\beta\gamma- k_{off,G}\cdot G\alpha_{GDP}G\beta\gamma$

(13) $dC_0/dt= -4\cdot k_{on}\cdot G\beta\gamma\cdot C_0+k_{off}\cdot C_1$

(14) $dC_1/dt=4\cdot k_{on}\cdot G\beta\gamma\cdot C_0-3\cdot k_{on}\cdot G\beta\gamma\cdot C_1- k_{off}\cdot C_1+ 2\cdot k_{off}\cdot C_2$

(15) $dC_2/dt=3\cdot k_{on}\cdot G\beta\gamma\cdot C_1-2\cdot k_{on}\cdot G\beta\gamma\cdot C_2- 2\cdot k_{off}\cdot C_2+3\cdot k_{off}\cdot C_3$

(16) $dC_3/dt=2\cdot k_{on}\cdot G\beta\gamma\cdot C_2-1\cdot k_{on}\cdot G\beta\gamma\cdot C_3- 3\cdot k_{off}\cdot C_3+4\cdot k_{off}\cdot C_4$

(17) $dC_4/dt=1\cdot k_{on}\cdot G\beta\gamma\cdot C_3- 4\cdot k_{off}\cdot C_4$

For models based on graded contribution of each Gβγ occupied state to channel activity the open probability was calculated according to:

(18)

$$P_o = P_{o,max}\cdot\sum_{1}^{4}\varphi_i\cdot\frac{C_i}{C_{total}}$$

where φ_i is the contribution factor of each occupied Gβγ state to open probability, and C_{total} is channel concentration ($C_{total}=\sum_{i=0}^{i=4} C_i$). φ_i values were adopted from Yakubovich et al.[1] and Berlin et al.[2] and based on data published by Ivanova-Nikolova et al. and Sadja et al.[4, 5].

For models based on concerted gating the open probability was calculated according to:

(19)

$$P_o = P_{o,max}\cdot\frac{C_4}{C_{total}}$$

These models are based on the same assumption as used in WTM model, i.e. only 4 Gβγ-occupied channel is available for opening.

In all models C_0-C_4 correspond to 0-4 Gβγ occupied state of the channel, k_{on} =1e7 $M^{-1}s^{-1}$ (similar to value utilized by Berlin at al. and in agreement with the diffusion limit[2, 6], $k_{off}=K_d/k_{on}$, μ is the cooperativity factor of Gβγ binding to each consecutive Gβγ occupied state[6]. $k_{on,G}$ =0.7e6 $M^{-1}s^{-1}$ and $k_{off,G}$ =0.0013 s^{-1} as reported by Sarvazyan et al. [7]. For simulation of response to expressed Gβγ initial values of [K_d $G\alpha_{endo}$, $G\beta\gamma_{endo}$+$G\beta\gamma_{expressed}$] were utilized for each consequtive run of differential equation system solution, thus generating matrix of [$G\beta\gamma_{expressed}$ P_o] values for each K_d. Differential equations systems were solved in Berkeley Madonna for Windows utilizing 4th order Runge-Kutta integration method. All systems were allowed to reach steady-state. The results of simulation were compared to experimental dose-response curves. For selection of optimal [K_d $G\alpha_{endo}$ $G\beta\gamma_{endo}$] values we utilized two criteria: a) the stability of G-protein concentration estimation as seen from Supplementary Fig. 8b – i.e. an optimal model is expected to generate stable estimation of G protein concentration over a wide range of tested K_d values, and b)

resemblance to superimposed dose-response by visual inspection. Simulations of all models are shown in Fig. 4g and Supplementary Fig. 8d,e.

Extracellular HA staining

Extracellular HA staining of the oocytes was performed as described[8]. Briefly, oocytes were fixated with 4% formaldehyde for 30 min, blocked in 5% milk in Ca^{2+}-free ND96 solution for 1 hour, incubated with mouse anti-HA antibody (1:333; Santa Cruz Biotechnology, Dallas, TX, USA) in 2.5% milk-Ca^{2+}-free ND96 for 1 hour, washed thrice, and incubated with DyLight405-conjugated anti-mouse antibody (KPL, Gaithersburg, MD, USA). Oocytes were then kept at 4°C in the dark in Ca^{2+}-free ND96 solution until imaged.

Supplementary Figures

Fig. S1

a

	$I_{\beta\gamma}$, µA	I_{basal}, nA			R_a			$R_{\beta\gamma}$			N
		mean	SEM	n	mean	SEM	n	mean	SEM	n	
GIRK2	2-4	64.2	7.1	49	8.2	0.8	49	67.3	7.9	52	7
	>4	137.7	19.2	48	5.1	0.4	48	68.9	9.3	31	5
GIRK2HA	3-10	69.8	16.4	16	5.7	0.7	16	78.0	9.6	21	3
	>10	348.7	34.0	23	4.9	0.7	23	49.4	7.1	18	3

b

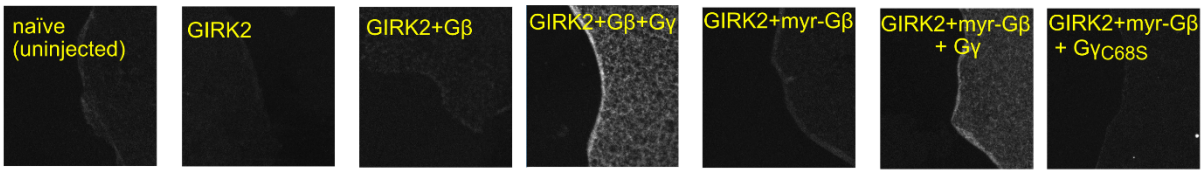

c

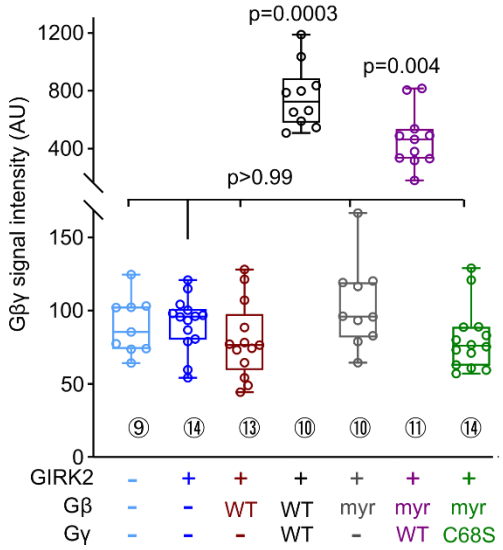

d

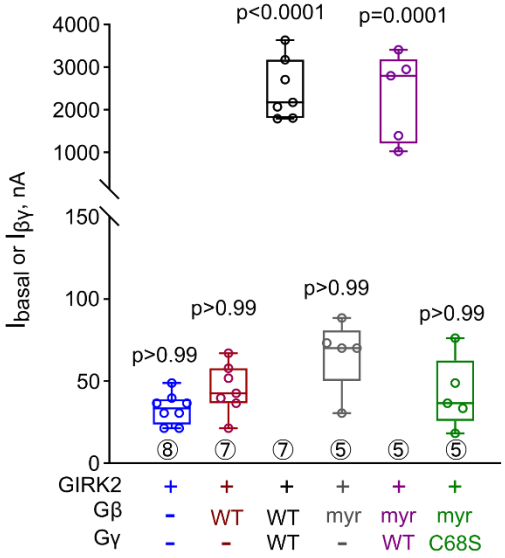

Supplementary Fig. 1. GIRK2 activation by ACh and Gβγ and the requirement for prenylation of Gγ. a, basal currents (I_{basal}), fold activation by ACh (R_a) and fold activation by Gβγ ($R_{\beta\gamma}$). The table shows summary of a series of experiments in which, on the same day, I_{basal} and I_{evoked} were measured in one group of oocytes expressing m2R and GIRK2, and $I_{\beta\gamma}$ in another group of expressing Gβγ, in 24 mM $[K^+]_{out}$ solution. m2R was expressed at 0.5-1 ng RNA, which ensures full maximal attainable I_{evoked}[2]. Gβ RNA was 5 ng and Gγ or Gγ-YFP were 1 or 2-2.5 ng, accordingly. Results were grouped according to $I_{\beta\gamma}$ as indicated in the 2nd column. **b**, examples of GMPs from oocytes injected with the indicated RNAs (YFP-GIRK2 was used in this experiment). RNAs injected were (in ng): YFP-GIRK2, 5; Gβ, 5; Gγ or $G\gamma_{C68S}$, 2. 1 ng m2R RNA was present in all groups except native oocytes. Note that, unlike Western blots, the Gβ antibody used here poorly recognized the endogenous oocyte's Gβ in GMP immunostaining[1]. Only $G\gamma_{WT}$ ensures the PM attachment of Gβ or myr-Gβ. Only a weak signal, reflecting the PM-attached endogenous Gβ, is observed in uninjected (native) oocytes or after expression of Gβ or myr-Gβ without Gγ. Note that myr-Gβγ is a functional protein that reaches PM and activates GIRK2 when expressed with $G\gamma_{WT}$. $G\gamma_{S68S}$ is unable to assist in enriching Gβγ in the PM. **c**, summary of Gβ measurements from **b**. Statistics: Kruskal-Wallis test on ranks followed by Dunn's multiple comparison vs. control group (native oocytes). **d**, Summary of GIRK currents measured in 24 mM $[K]_{out}$ in the same experiment as a, b. Statistics: as in c. In **c** and **d**, number of cells tested is shown near data boxes (encircled numbers).

Fig. S2

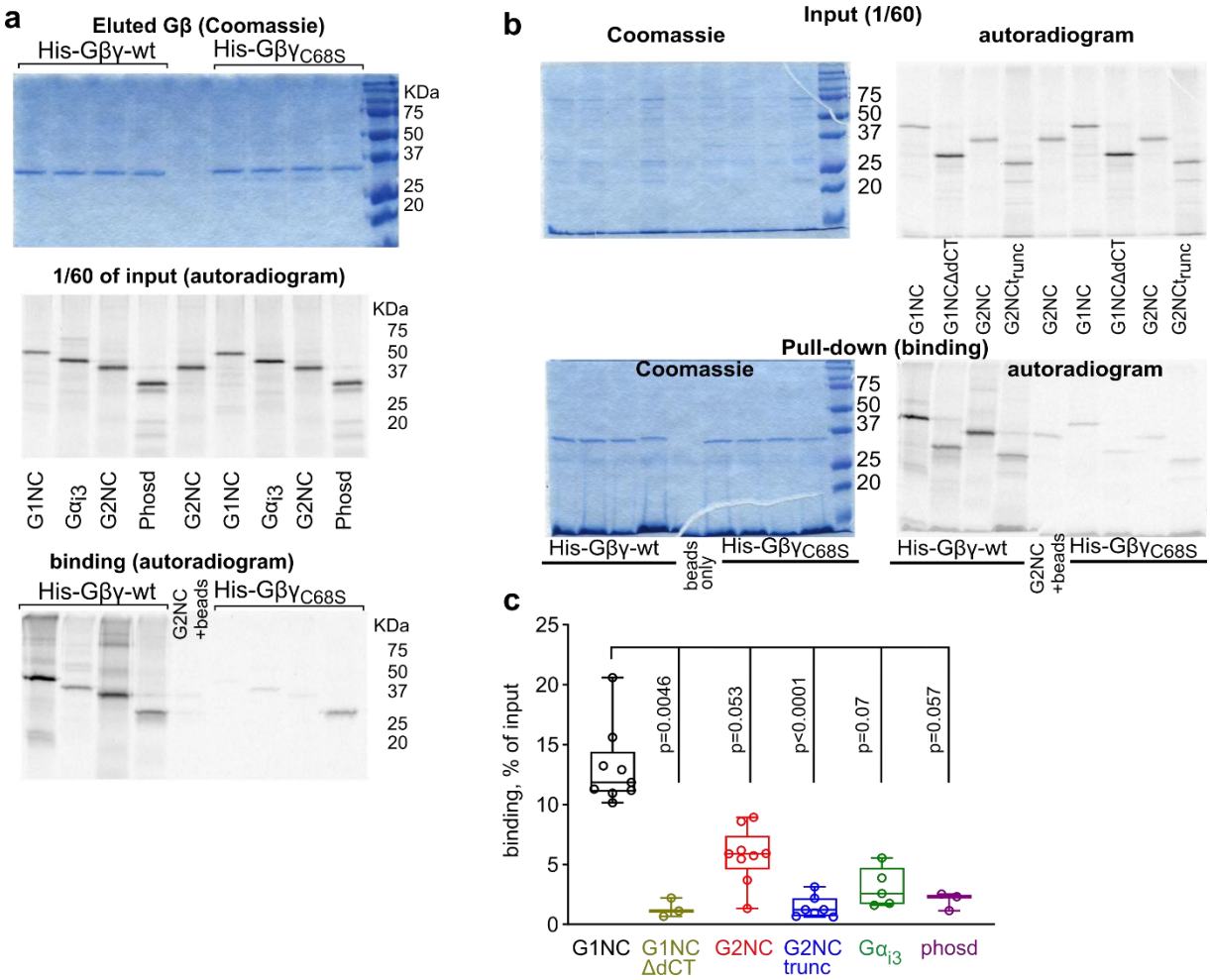

Supplementary Fig. 2. Differences in binding of $G\alpha_{i3}$-GDP, phosducin and cytosolic segments of GIRK1 and GIRK2 to WT Gβγ and non-prenylated Gβγ. a, the full gel of the experiment shown in Fig. 1c. **b**, a representative experiment comparing binding of *ivt* full-length G1NC and G2NC and their truncated versions, $G2NC_{trunc}$ and $G1NC_{\Delta dCT}$, to WT His-Gβγ and non-prenylated His-$G\beta\gamma_{C68S}$. Upper and lower images represent two separate gels. Left images show Coomassie staining of proteins in reaction mix (1/60 of total; "input (1/60)", top) and eluted proteins (binding; bottom). Right images show autoradiograms of the same gels. **c**, comparison of binding of the various interactors to $G\beta\gamma_{WT}$. Shown are the same data as in Fig. 1d but without the binding to $G\beta\gamma_{C68S}$. Statistics: Kruskal-Wallis test followed by Dunn's multiple comparison test vs. control (G1NC).

Fig. S3

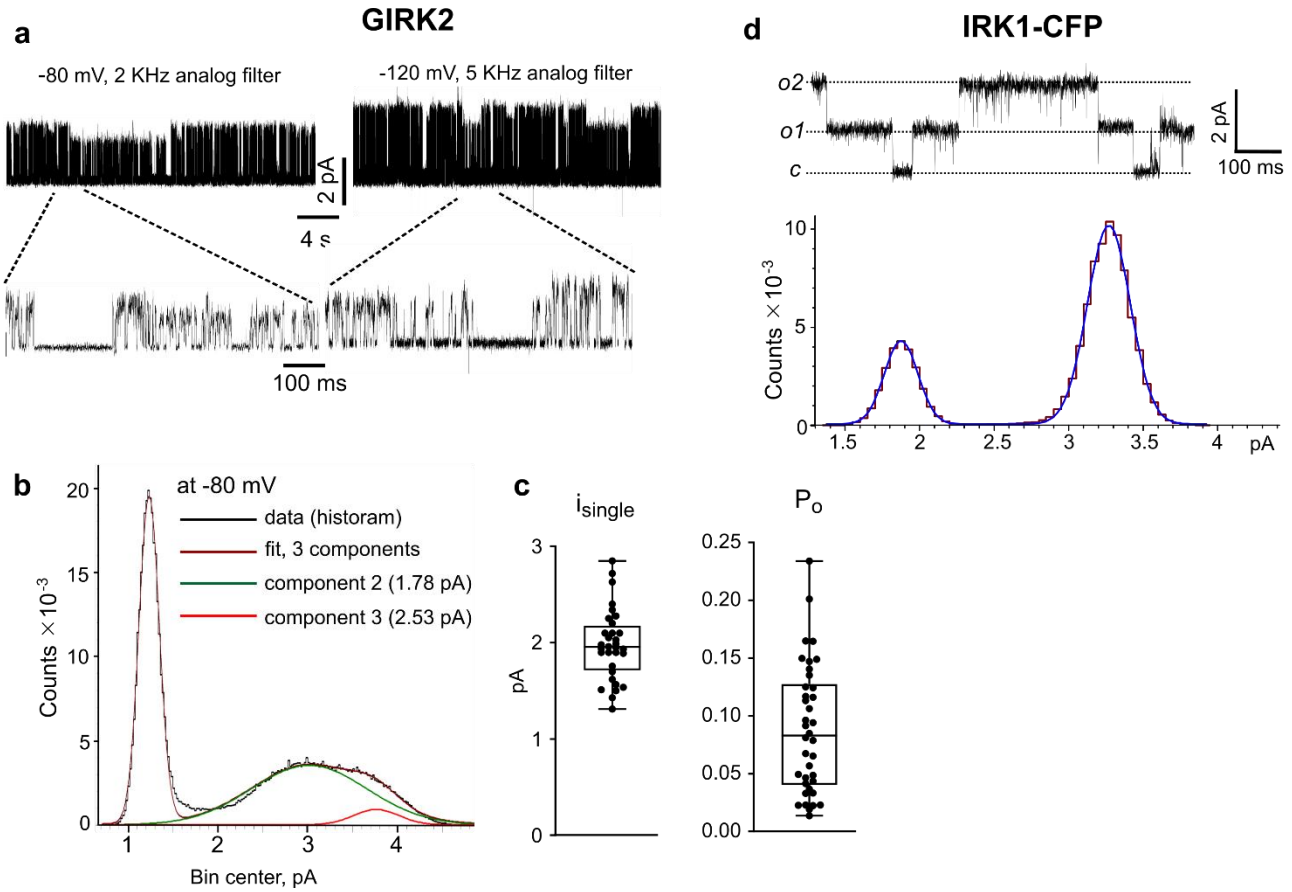

Supplementary Fig. 3. Characterization of single-channel parameters of GIRK2 and IRK1-CFP. a-c, analysis of a cell-attached record from an oocyte injected with 25 ng of the anti-GIRK5 oligonucleotide and the following RNAs (in ng/oocyte): GIRK2, 0.017; m2R, 2; Gβ, 5; Gγ, 1. The patch contained one active channel, as assessed from lack of overlaps during the ~10-minute record. **a,** representative segments of the record at -80 mV and -120 mV acquired at 20 KHz with either 2 KHz or 5 KHz analog filter, as indicated. Inward K^+ currents are shown as upward deflections. **b,** all-points amplitude histogram of the left record from **a** (at -80 mV). The left peak corresponds to the background noise. The parameters of the 3 components of the Gaussian fit were: μ_1=1.23 pA, σ_1=0.11 pA; μ_2=3.01 pA, σ_2=0.64 pA; μ_3=3.76 pA, σ_3=0.25 pA. The two components of the fit corresponding to the two subconductance levels are shown with green and red lines. Two conductance levels (substates) have been observed in a minority of GIRK2 records. The proportion of the two levels varied among patches, but usually either the larger or the smaller one was predominant (see, for example, Fig. 3c,d). In most cells the channel current in all-point amplitude histograms was well fitted with one Gaussian component. **c,** single channel parameters of GIRK2. P_o was calculated from 2 to 4 min segments of idealized traces from patches containing 1 to 3 channels. The weighted averaged i_{single} was calculated from all-points histograms. Amplitude analysis was limited to patches with P_o>0.05 to avoid filtering artifacts with very short openings. **d**, section of a record from an oocyte injected with 5 pg IRK1-CFP RNA. Holding potential was -80 mV. Two channels were present; *c* denotes closed channel current level, *o1* – one open channel, *o2* – two open channels' current. *Bottom*, all-points histogram of a section of the record from the same patch, fitted with a two-component Gaussian for determining the single channel amplitude, i_{single}. In this patch, P_o was 0.81 and i_{single} was 1.39 pA. A summary of single channel parameters for all channels used here is presented in Supplementary Table 3.

Fig. S4

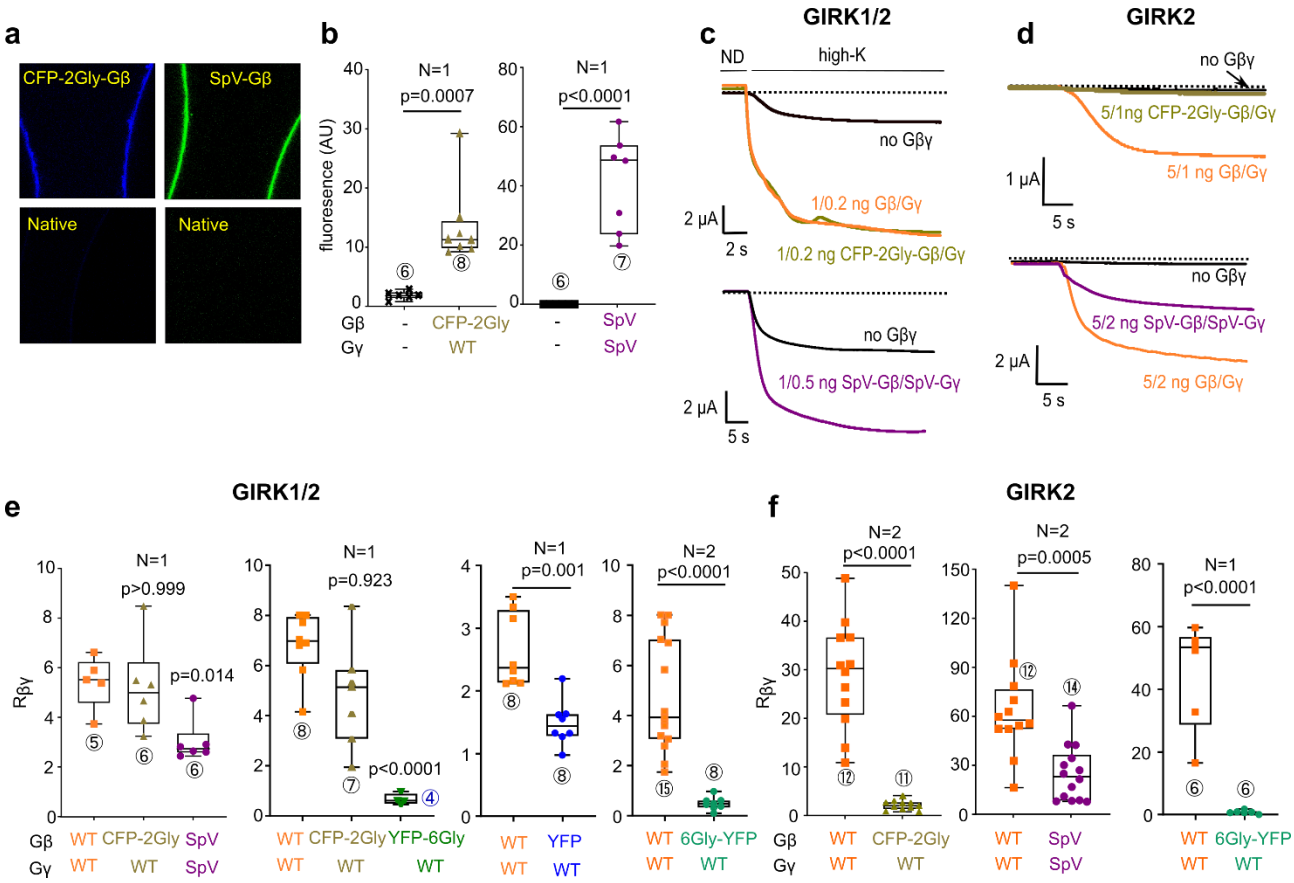

Supplementary Fig. 4. xFP-fused Gβ constructs perform poorly in activating GIRKs. a, examples of confocal images of oocytes injected with GIRK2 (2 ng RNA) and RNAs of CFP-2Gly-Gβ (1 ng) and Gγ (0.4 ng), or SpV-Gβ (1 ng) and SpV-Gγ (0.5 ng). Both SpV-Gβγ and CFP-2Gly-Gβ were expressed in the plasma membrane. The intensity of images from the CFP-2Gly-Gβ experiment (both native and Gβ-expressing oocytes) was enhanced 2-fold using Corel PhotoPaint, for better visibility. **b,** summary of expression levels of CFP-2Gly-Gβ and SpV-Gβγ in whole oocytes, compared to the background fluorescence of native oocytes. AU, arbitrary units. Unpaired t-test was used for CFP-2Gly-Gβ and Mann-Whitney test was used for SpV-Gβγ. **c, d**, representative whole-cell currents in oocytes expressing GIRK1/2 (**c**) and GIRK2 (**d**). The amounts of injected RNAs were: GIRK1, 0.05 ng; GIRK2, 0.05 ng as heterotetramer and 2 ng as homotetramer. The amounts of Gβ or xFP-Gβ were: 1 ng when coexpressed with GIRK1/2 and 5 ng with GIRK2. The record started in a low-K^+ external solution (ND96; ND) which was then switched to high-K solution (24 mM $[K^+]_{out}$). **e, f**, summary of fold-Gβγ activation ($R_{\beta\gamma}$) by Gβγ vs. the various xFP-labeled Gβ with WT Gγ (except for SpV Gβγ). Gβ RNA doses were as in **c**, except Gβ-6Gly-YFP, which was 5 ng RNA/oocyte in all cases. Of all constructs, only CFP-2Gly-Gβ activated GIRK1/2 similarly to Gβγ (**e**), but it did not activate GIRK2 (**f**). SpV-Gβγ activated both GIRK2 and GIRK1/2 but significantly less than $G\beta\gamma_{WT}$. With Gβ-6Gly-YFP (YFP fused to Gβ's C terminus via a 6-glycine linker), no activation at all was seen with GIRK2 (**f**, right panel), and GIRK1/2 was even reduced relative to its I_{basal} (**e**, right panel; $R_{\beta\gamma}$=0.49±0.09). Statistical analysis included the Shapiro-Wilk normality test, and the following analysis was done using the appropriate tests as detailed in Methods. Number of cells (encircled) is shown near the columns, and number of experiments is shown as N.

Fig. S5

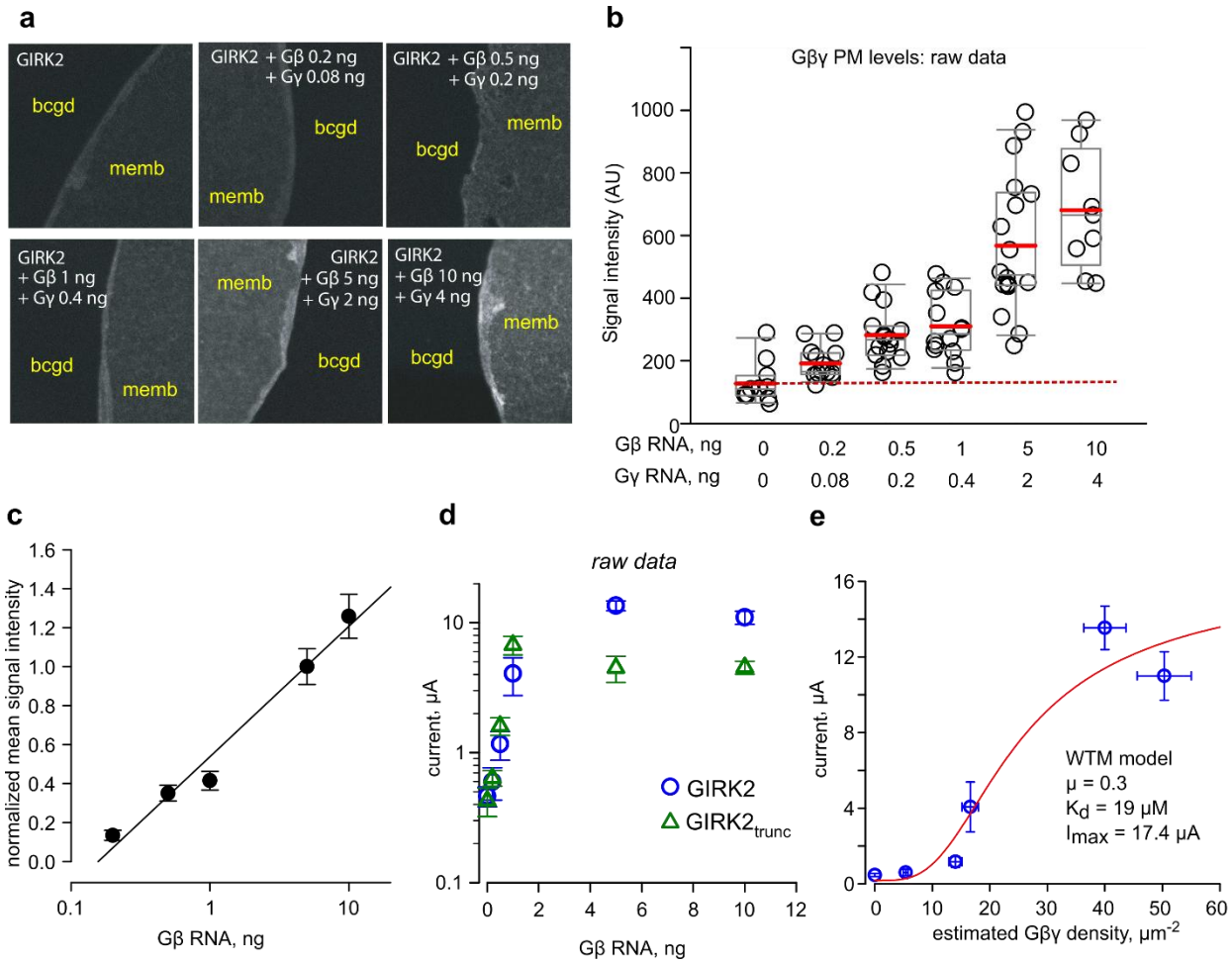

Supplementary Fig. 5. Dose-dependent Gβγ activation of GIRK2 and GIRK2$_{trunc}$. Whole-cell currents of the two constructs were compared in one experiment. **a,** representative images of giant plasma membrane patches (GMP) stained with Gβ antibody (Santa Cruz, SC-378). GIRK2 channel (2 ng RNA/oocyte) was present in all groups, and Gβ and Gγ RNAs were coinjected in the indicated amounts. bckg, background; memb, membrane. **b**, summary of measurements of Gβγ in GMPs. AU, arbitrary units. Nine to 18 GMPs were measured with each Gβγ dose. Boxes show 25-75 percentiles and whiskers 5-95 percentiles. Red lines within the boxes show the mean and the grey lines the median values. **c**, relation between the amount of injected Gβ RNA and Gβ protein measurement in the GMPs. Circles show mean±SEM from the same measurements shown in b. In this experiment, the surface levels of expressed Gβγ were empirically found to be linearly related to log[Gβ RNA dose]. Data are shown as mean±SEM, with linear regression line. Net values of expressed Gβγ, after subtraction of the average background signal measured in native oocytes, were normalized to the signal seen with 5 ng Gβ RNA. **d**, whole-cell GIRK2 and GIRK2$_{trunc}$ (2 ng RNA/oocyte) currents measured in 96 mM K^+ solution. GIRK2$_{trunc}$ lacks the first 51 amino acid residues (a.a.) of the cytosolic N-terminus and the last 24 a.a. of the CT. **e,** dose-dependent activation of GIRK2 by Gβγ. The density of expressed Gβγ in the PM obtained with 5 ng Gβ RNA was assumed to be 40 molecules/μm^2 (as in Fig. 3 and close to the average 35 molecules/μm^2 from qWB data, Supplementary Table 4), and Gβγ PM densities for other RNA doses were calculated based on the regression line from Fig. 2c. The circles show mean estimated Gβγ density (±SEM) on the X axis (n=8-18) and mean±SEM current on the Y-axis (n=7-13). The parameters of WTM model fit with fixed μ=0.3 (red line) are shown in the inset.

Fig. S6

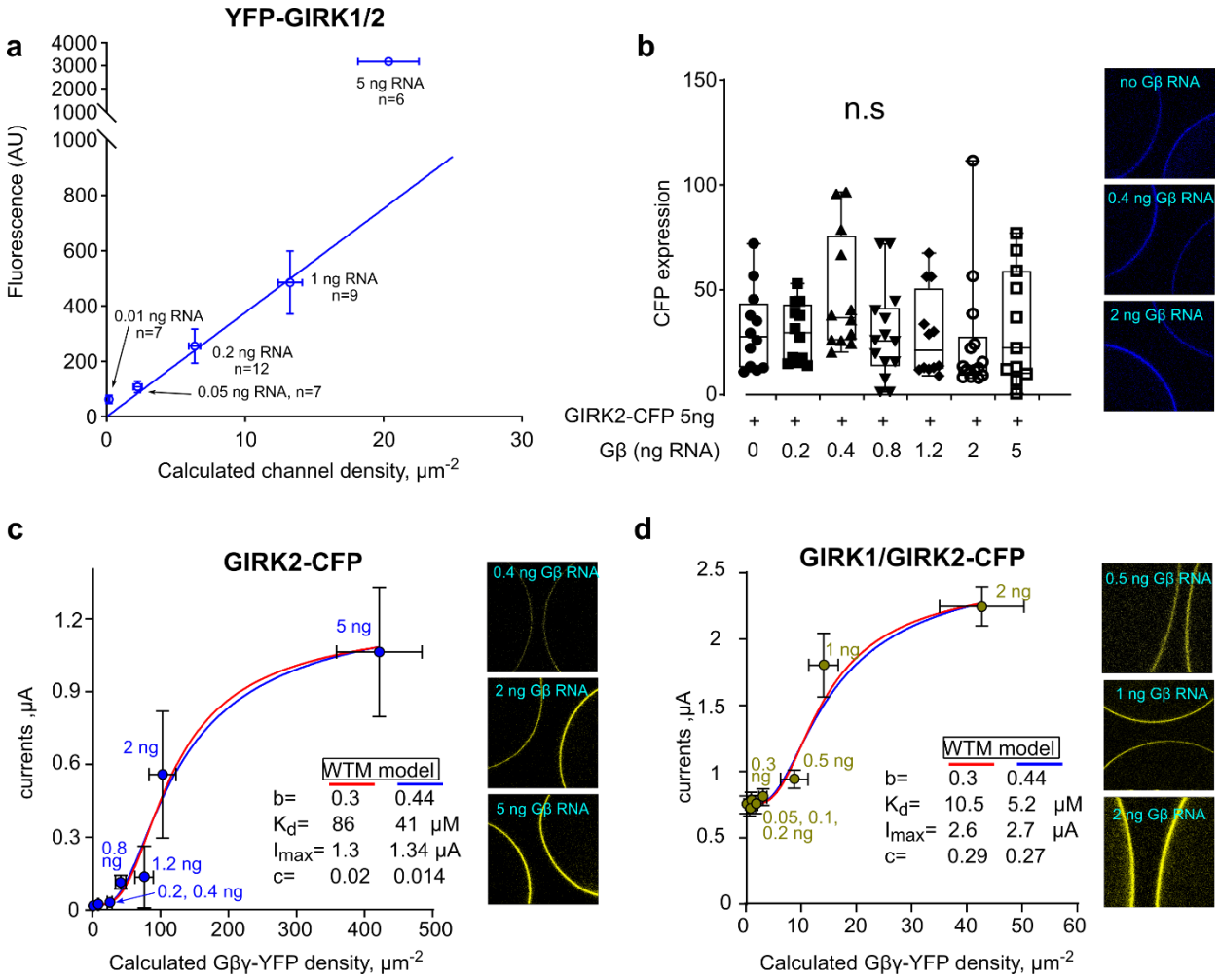

Supplementary Fig. 6. Testing linear range of CE calibration (a) and dose-dependent activation of GIRK2-CFP and GIRK1/2-CFP by coexpressed Gβ·$_{YFP}$Gγ (b-d). a, testing linearity of surface fluorescence of YFP vs. surface density of YFP-GIRK1/2 in a wide range of channel subunits' RNA (0.01-5 ng/oocyte of each subunit, shown near each point) coexpressed with Gβγ (5:1 ng RNA). YFP fluorescence was measured in 10 oocytes in each group; for current measurements, n is shown near the points. Data are shown as mean±SEM. The linear regression line was drawn via zero and all data points except 5 ng RNA (we never used more than 1 ng in GIRK1/2 experiments). Deviations from linearity were observed in all 3 experiments where 5 ng GIRK1/2 RNAs were tested. **b-d**, data are from one experiment. Calibration was done with YFP-GIRK1/2 coexpressed with Gβγ (5:1 ng RNA; not shown). **b**, GIRK2-CFP (5 ng RNA/oocyte) was expressed with Gβ·$_{YFP}$Gγ (2:1 ratio Gβ to YFP-Gγ RNA), and its expression was measured from confocal images of intact oocytes (right panel). Coexpression of Gβ·$_{YFP}$Gγ did not significantly affect the expression of GIRK2-CFP in the PM. Boxes show 25-75 percentiles, whiskers the full data range, lines within the boxes show the median. Statistics: Kruskal-Wallis ANOVA followed by Dunn's multiple comparison test. **c**, dose-dependent activation of GIRK2-CFP by Gβ·$_{YFP}$Gγ. The expression of Gγ-YFP was measured in 11-14 intact oocytes for each group (exemplary images are in the right panel). GIRK currents were measured in 8-10 oocytes. WTM fits with μ=0.3 (red line) and μ=0.44 (blue line) are shown. **d,** dose-dependent activation of GIRK1/GIRK2-CFP (50 pg RNA/oocyte of each subunit) by Gβ·$_{YFP}$Gγ. Gβ·$_{YFP}$Gγ expression in the PM was measured from 9-12 intact oocytes for each Gβ·$_{YFP}$Gγ dose. Representative images are shown on the right. GIRK currents were measured in 5-18 oocytes. WTM fits with μ=0.3 (red line) and μ=0.44 (blue line) are shown. This result was not included in the summary of Fig. 4h and Supplementary Table 6, because GIRK2-CFP showed lower sensitivity to Gβγ than WT GIRK2, as judged both by the small magnitude of $I_{\beta\gamma}$ and the high K_d.

Fig. S7

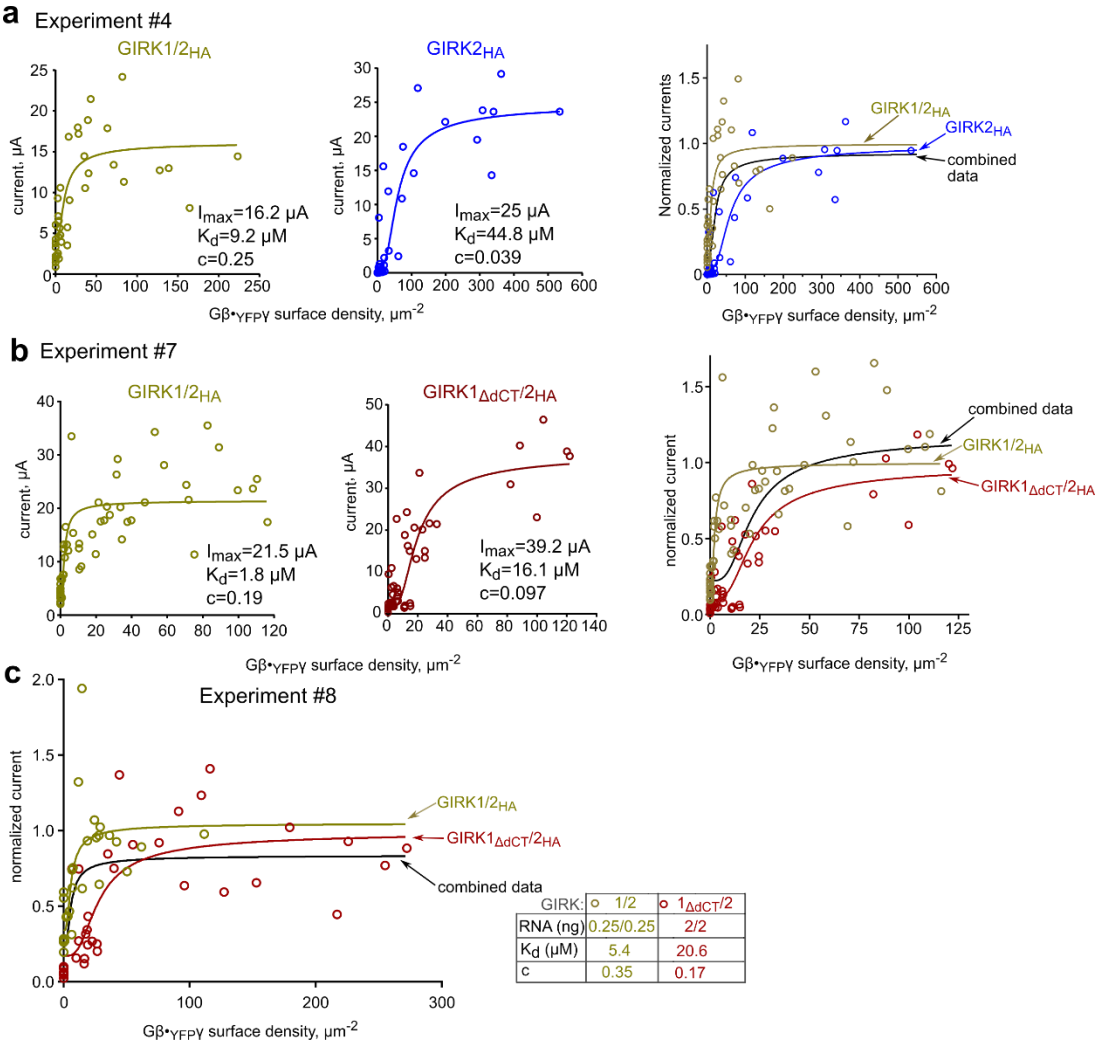

Supplementary Fig. 7. GIRK2 and GIRK1$_{\Delta dCT}$ show lower apparent affinity to Gβγ than GIRK1/2: raw data in individual oocytes and WTM fits. Data were fitted with the WTM model with μ=0.3; fit parameters are in the panels. **a,** activation of GIRK1/2$_{HA}$ (left; 0.25 ng RNA of each subunit) and GIRK2$_{HA}$ (middle; 5 ng RNA/oocyte) by Gβ·$_{YFP}$Gγ (0.2-10 ng Gβ, 5:1 Gβ:Gγ RNA). Right panel: WTM fits of currents normalized to maximal $I_{βγ}$ (I_{max}, Supplementary Table 6) and fitted as in Fig. 4 but, in this case, we also included a comparison with the combined data (experimental points for both channel compositions) corresponding to null hypothesis (no difference between the dose-response curves). The analysis was done according to GraphPad guide: https://www.graphpad.com/guides/prism/latest/curve-fitting/reg_comparing_fits_with_anova.htm. Briefly, the data for two channel compositions were fitted separately and together (combined data) to Eq. 5. The K_d, n and the SEM parameter of goodness of fit from the three fits were compared using one-way ANOVA and the p value was extracted from F-test and AICc test reports. The differences between the three sets were significant, F(2,162)=146460, p<0.0001 by F test; P<0.01 by AIC test). **b**, GIRK1/2$_{HA}$ (left;, 0.25 ng RNA/oocyte) and GIRK1$_{\Delta dCT}$/2-HA (middle; 2 ng RNA/oocyte) were activated by coexpression of Gβ (0.1-5 ng RNA/oocyte) and YFP-Gγ in 2:1 RNA ratio. Right panel: WTM fits of normalized currents (as in **a**) fitted to the WTM model (μ = 0.3) for GIRK2$_{HA}$, GIRK1/2$_{HA}$, and the combined data. The differences between fits were significant: F(2,206)=28358, P<0.0001; P<0.01 by AIC test. **c**, dose-dependent activation of GIRK1/2$_{HA}$ and GIRK2$_{HA}$ by Gβ·$_{YFP}$Gγ (experiment #8). Analysis and presentation of data are as the right panels in a and b. The differences between the fits were significant, F(2,116)=24243, P<0.0001. In a pairwise comparison between GIRK1/2$_{HA}$ and GIRK2$_{HA}$, the difference in K_d was significant: F(1, 58)=12.15, p=0.0009.

Fig. S8

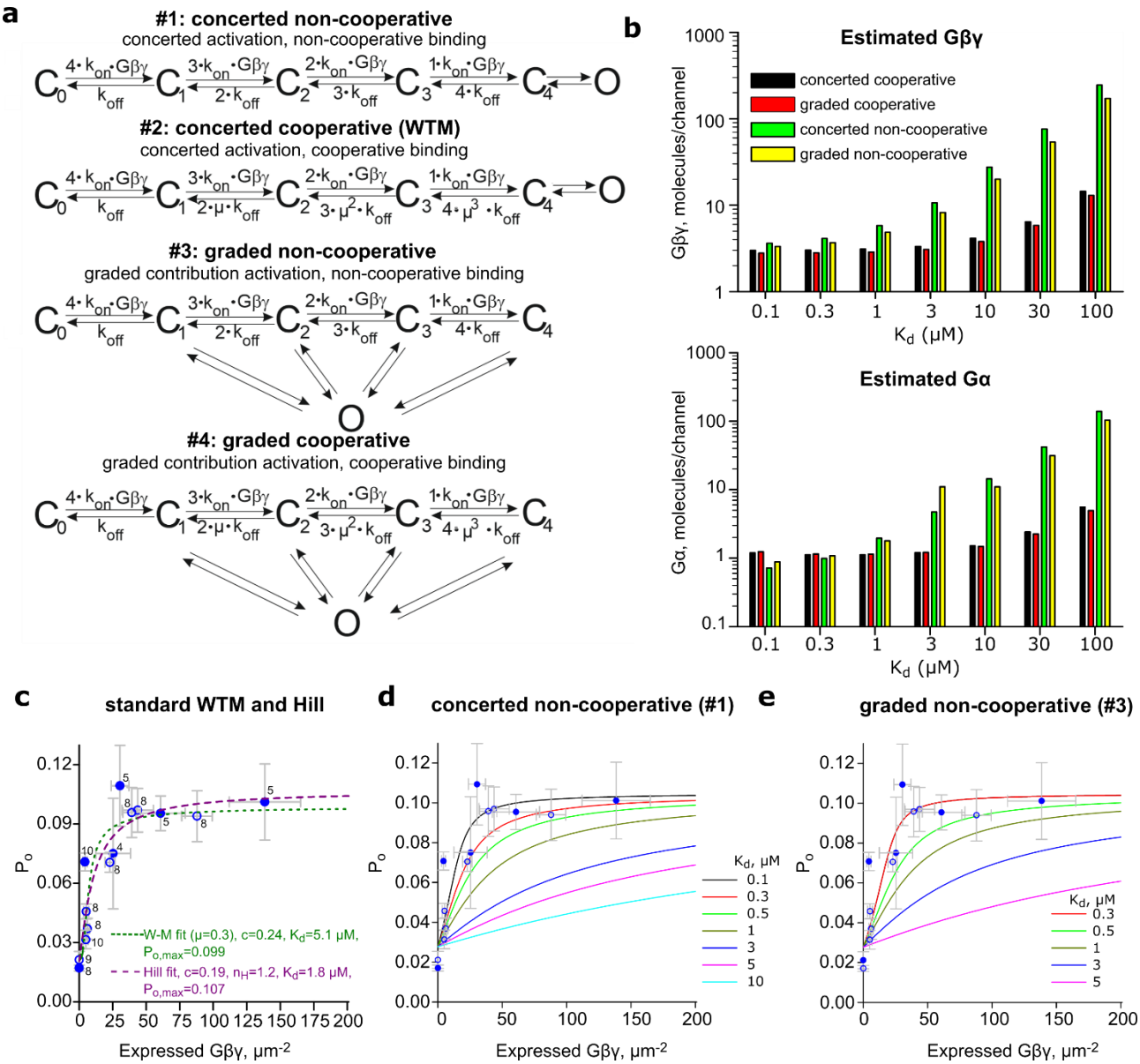

Supplementary Fig. 8. Modeling basal and Gβγ-evoked GIRK1/2 activity. a, the four kinetic models for Gβγ activation of GIRK1/2. Up to four Gβγ bind sequentially to the activation sites. In concerted models, the channel opens only when all four sites are Gβγ-occupied. In graded contribution models, occupation of the first site leads to opening, and binding to each additional site increases the P_o in a more-than-additive manner[1]. In cooperative models, each subsequent Gβγ binds with a higher affinity than the previous one. In the non-cooperative models, the affinity of Gβγ to each binding site is the same. **b**, amounts of available basal endogenous Gα and Gβγ that determine I_{basal} and I_{evoked}, per channel, were calculated with each of the kinetic models for a range of K_d (see Supplementary Methods). **c**, data from two experiments with GIRK1/2_{HA} (Supplementary Table 6), #4 (closed symbols) and #7 (open symbols; experiment of Fig. 4d), were pulled and fitted to the standard WTM and Hill models. Each point shows mean±SEM of P_o (Y-axis) vs. Gβ·$_{YFP}$γ surface density (X-axis). Numbers of cells are shown near the data points. The whole-cell current at each Gβγ dose was expressed as fraction of the maximal current obtained in WTM fit (24 and 13.4 μA in experiments #4 and #7) and transformed into P_o assuming $P_{o,max}$=0.105 (Supplementary Table 3). **d**, **e**, simulated Gβγ dose-response curves for the concerted and graded non-cooperative models, with a range of K_d values. The basal P_o of ~0.3 is not a fitted value but emerges from basal levels of Gβγ and Gα (as shown in **b**). The data points are the same as in **c.** The simulations best align with data with K_d between 0.1-0.5 μM.

Fig. S9

a

B1 RKFGDDYQVVTTSSSGSGLQPQGPG
C1 DYQVVTTSSSGSGLQPQGPGQGPQQ
D1 TTSSSGSGLQPQGPGQGPQQQLVPK
E1 GSGLQPQGPGQGPQQQLVPKKKRQR
F1 PQGPGQGPQQQLVPKKKRQRFVDKN
G1 QGPQQQLVPKKKRQRFVDKNGRCNV
H1 QLVPKKKRQRFVDKNGRCNVQHGNL
I1 KKRQRFVDKNGRCNVQHGNLGSETS

b

```
hGIRK2   1     makltesm tnvlegdsmd qdvespvaih qpklpkqard dlprhisrdr tkrkiqryvr kdgkcnvhhg nvretyrylt  78
mGIRK2A  1   mtmakltesm tnvlegdsmd qdvespvaih qpklpkqard dlprhisrdr tkrkiqryvr kdgkcnvhhg nvretyrylt  80

hGIRK2   79  difttlvdlk wrfnllifvm vytvtwlffg miwwliayir gdmdhiedps wtpcvtnlng fvsaflfsie tettigygyr  158
mGIRK2A  81  difttlvdlk wrfnllifvm vytvtwlffg miwwliayir gdmdhiedps wtpcvtnlng fvsaflfsie tettigygyr  160

hGIRK2   159 vitdkcpegi illliqsvlg sivnafmvgc mfvkisqpkk raetlvfsth avismrdgkl clmfrvgdlr nshiveasir  238
mGIRK2A  161 vitdkcpegi illliqsvlg sivnafmvgc mfvkisqpkk raetlvfsth avismrdgkl clmfrvgdlr nshiveasir  240

hGIRK2   239 aklikskqts egefiplnqt dinvgyytgd drlflvspli isheinqqsp fweiskaqlp keeleivvil egmveatgmt  318
mGIRK2A  241 aklikskqts egefiplnqt dinvgyytgd drlflvspli isheinqqsp fweiskaqlp keeleivvil egmveatgmt  320

hGIRK2   319 cqarssyits eilwgyrftp vltledgfye vdynsfhety etstpslsak elaelasrae lplswsvssk lnqhaelete  398
mGIRK2A  321 cqarssyits eilwgyrftp vltledgfye vdynsfhety etstpslsak elaelanrae lplswsvssk lnqhaelete  400

hGIRK2   399 eeeknleeqt erngdvanle neskv 423
mGIRK2A  401 eeeknpeelt erng             414
```

Supplementary Fig. 9. Illustration of analysis of peptide array data and comparison of hGIRK2 with mGIRK2A. a, the method used to designate the approximate boundaries of Gβγ-binding regions from peptide array scans, exemplified with the GIRK1 NT Gβγ-binding region (highlighted in yellow). The boundaries were arbitrarily defined before the last 10 a.a. of the first 25-mer Gβγ-labeled peptide, and after the first 10 a.a. of the last Gβγ-labeled peptide. In cases when the starting or the last peptide of the array bound Gβγ, 5 N-terminal a.a. were not counted as part of the binding site. **b**, alignment of a.a. sequences of mouse GIRK2A (mGIRK2A) used in most experiments in this report, and hGIRK2 used for the peptide arrays. There are 2 a.a. differences (highlighted in yellow). In addition, hGIRK2 is 2 a.a. shorter in its N terminus and contains 11 a.a. in its dCT not present in mGIRK2A. The last a.a. of mGIRK2A (G414) corresponds to G412 of hGIRK2.

Fig. S10

a

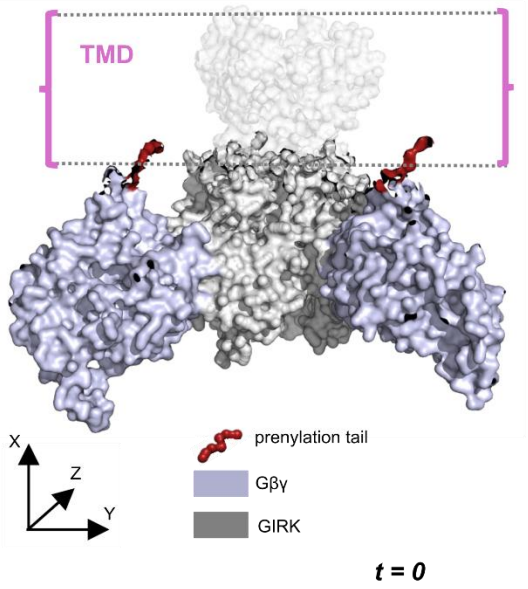

c **Interactions of $G\gamma_{prenyl}$ with Gβ residues (% of simulation run time)**

	Non-truncated G2NC		$G2NC_{trunc}$	
Run #	% Gβ (a.a. 314-338) interactions	Top a.a. involved	% Gβ (a.a. 314-338) interactions	Top a.a. involved
1	2.12	W338 (99%), K336 (1%)	0.7	W338 (99%)
2	2.22	W338 (95%), F334 (5%)	0.8	W338 (95%), F334 (5%)
3	0.4	W338 (100%)	0.12	W338 (100%)
4	0.4	W338 (99%)	0.62	W338 (99%)
5	0.38	W338 (100%)	0.13	W338 (98%)
6	0.56	W338 (99%), F334 (1%)	0.72	W338 (99%)
7	0.16	W338 (97%), K336 (3%)	0.66	W338 (98%)
8	0.18	W338 (99%)	0.31	W338 (99%)
9	0.5	W338 (99%)	0.82	W338 (99%)
10	0.01	W338 (71%), K336 (47%)	0.43	W338 (48%), K336 (34%), F334 (17%)
Total	**26.3**		**53.1**	

b

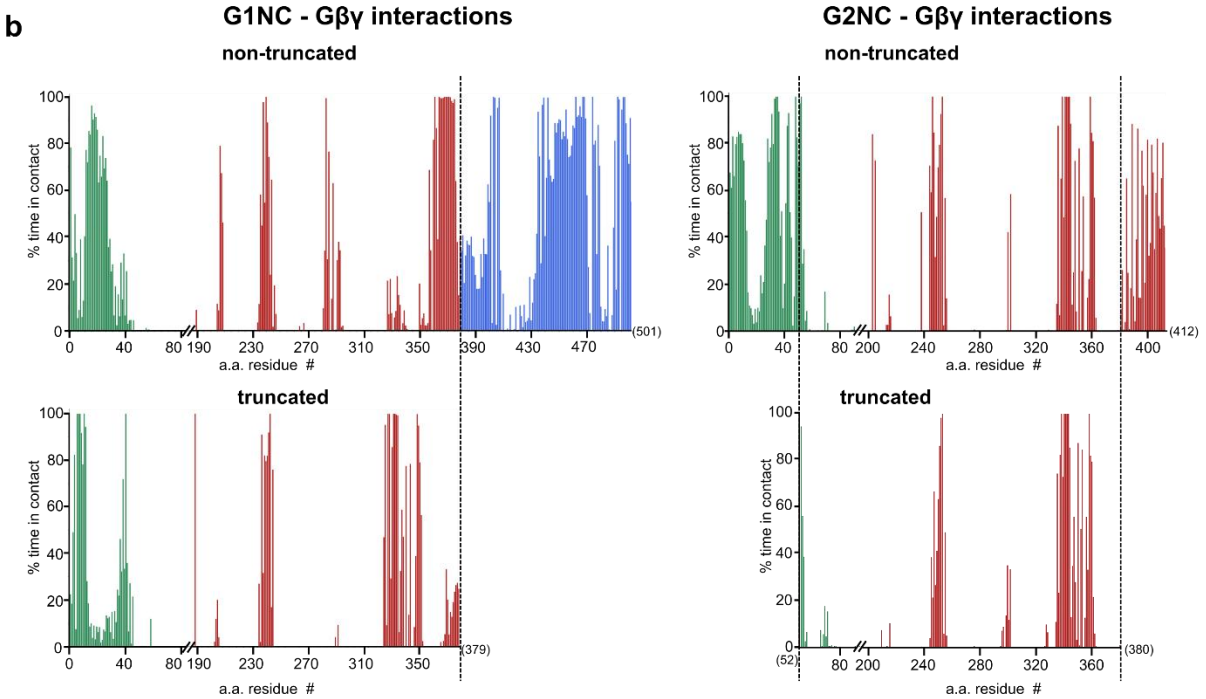

Supplementary Fig. 10. MD simulations of binding of prenylated Gβγ to full-length and truncated G1NC and G2NC, and of $G\gamma_{prenyl}$ to Gβ. a, coarse-grained models of G1NC, G2NC, and their truncated versions, which include the bound Gβγ subunits and the prenylation tail ($G\gamma_{prenyl}$). The image shows the experimental system, exemplified for the GIRK2/Gβγ complex at the beginning of the MD simulation (t=0). **b**, histograms showing % of time spent by each a.a. within full-length (non-truncated) and truncated G1NC and G2NC in contact with Gβγ across all runs. **c**, summary of interactions of $G\gamma_{prenyl}$ with the hydrophobic residues of Gβ in the G2NC-Gβγ system.

Fig. S11

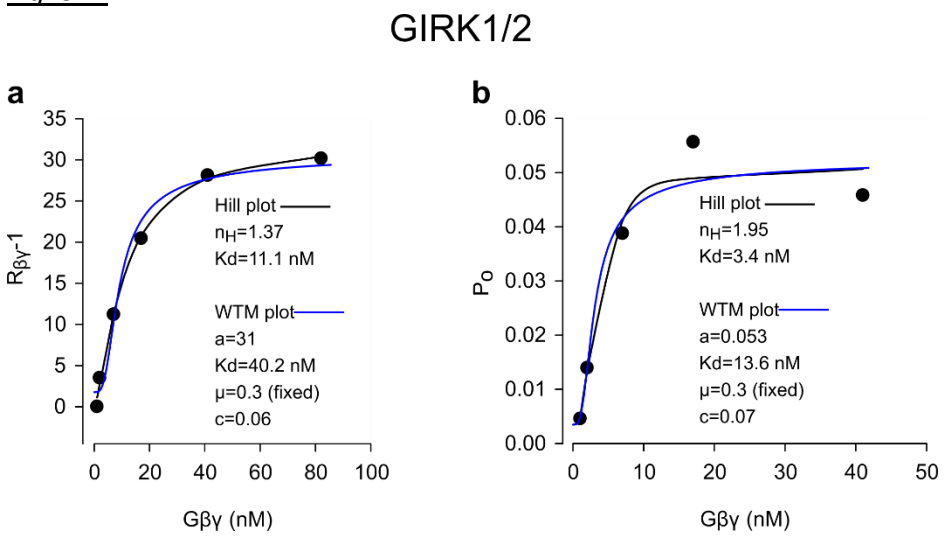

Supplementary Fig. 11. Dose-dependent activation of GIRK1/2 by Gβγ added to the bathing solution in excised patch experiments. Original data reported in Peleg et al., 2002[9] were fitted to Hill and WTM models. **a**, results from multichannel patches (>3 channels/ patch; n=4-8 patches for each point). $R_{\beta\gamma}$ is calculated as (NP_o at the peak of activation by Gβγ)/(NP_o during the last minute before addition of Gβγ). Channel activity is presented as $R_{\beta\gamma}$-1. **b**, results from patches with 1-3 channels where the exact P_o could be calculated (n=3-8 except the lowest does of Gβγ, where n=1). For additional details, see Fig. 7 in Peleg et al. 2002[9]. Note that basal activity of GIRK1 these patches was 3-7% of maximal P_o, which is lower than in our usual whole-cell records. There are two reasons for that: first, activation by Gβγ is stronger for low expression levels of GIRK1/2[1, 9] (to achieve low channel density for single-channel recordings, we injected 5-20 pg RNA vs. 50-250 pg in standard whole-cell experiments, e.g. Fig. 3, Supplementary Fig. 3). Second, Gβγ was applied 3 min after excision when basal activity already decays by ~50% compared to cell-attached mode (Fig. 5). Comparing WTM fits of GIRK1/2 activation by coexpressed Gβγ in whole oocytes (K_d=5.5 μM, Fig. 4f) and by purified Gβγ in excised oocyte's patches[9] (K_d=13-40 nM) suggests a partition coefficient between 140 and 425.

Supplementary Tables

Supplementary Table 1. Dissociation constants of Gβγ effectors, including GIRKs.

Gβγ-binding protein	K_d	Method and Gβγ used	Ref.
$G\alpha^{GDP}$ (various Gα proteins)	0.2-27 nM	Fluorescent flow cytometry with bovine brain Gβγ in detergent solutions	10
PH-PLCγ1 Ras-GRF SOS-PH	318 nM 108 nM 208 nM	SPR; **prenylated** $G\beta_1\gamma_1$	11
KCTD12 (H1 domain)	185 nM	Isothermal titration calorimetry; **non-prenylated** $G\beta_1\gamma_2$	12
D2 (in I-II linker of $Ca_V2.1$ α1 subunit) AID, as above	24 nM 63 nM	Pull-down of *ivt* $G\beta_1\gamma_2$ (presumably prenylated) by GST-fused segments of I-II linker on glutathion affinity resin	13
phosducin	42 nM	SPR; **prenylated** $G\beta_1\gamma_1$	14
GRK2 (βARK1)	25 nM	Purified **prenylated** $G\beta_1\gamma_2$ added to GRK2 affinity beads (not in lipid phase)	15
PLCβ2	3.2 μM	lipid bilayers, binding curve from FRET, **prenylated** Gβγ concentration in membrane was estimated directly	16
cardiac I_{KACh} GIRK1 GIRK4	55 nM 125 nM 50 nM	Immunoprecipitated GIRKs bound to Gβγ on the surface of immunobeads; competition with radiolabeled **prenylated** Gβγ added in detergent solution.	17
GIRK4, short C-terminal peptide (209-225)	60 nM	competition of synthetic peptides with atrial GIRK1/4 for binding of **prenylated** $G\beta_1\gamma_2$ in detergent solution	18
GIRK4 C-terminus	≤790 nM	SPR; **prenylated** $G\beta_1\gamma_2$	19
GIRK1 cytosolic domain, N- and C-terminally truncated	250 μM	NMR in solution; **non-prenylated** $G\beta_1\gamma_2$	20
Purified $GIRK2_{trunc}$	1.9 mM (~300 μM in high Na^+)	lipid bilayers, dose-response of channel's activity, **non-prenylate**d $G\beta_1\gamma_2$	21

Abbreviations: AID, α-subunit binding domain; βARK1, β-adrenergic receptor kinase 1; GRK2, G protein-dependent receptor kinase 2; NMR, nuclear magnetic resonance; PH, plekstrin homology domain; PLC, phospholipase C; Ras-GRF, Ras-specific guanine nucleotide exchange factor; SOS, son-of-sevenless protein; SPR, surface plasmon resonance.

Supplementary Table 2. The values of K_d calculated for sequential cooperative Gβγ binding to GIRK2.

K_{d1}, K_{d2}, K_{d3} and K_{d4} are K_d values, in μM, for the binding of the 1st, 2d, 3d and 4th Gβγ, respectively. The numbers in yellow rectangle correspond to estimates of Wang et al.[21] with 0 to 4 bound Na^+ ions per GIRK2 channel. The values of K_{d1} in the following rows have been chosen arbitrarily for illustration purposes and are calculated for the case of constant Na^+ concentration with cooperativity factor for Gβγ sequential binding (μ) fixed at 0.3. For calculation of Na^+-dependent changes the cross-cooperativity coefficient between Na^+ and Gβγ was 0.63[21]. Calculations were done according to the WTM model (Eqn. 5, Methods).

Na ions/ channel	K_{d1}	K_{d2}	K_{d3}	K_{d4} (μM)
0	1900	570	171	51
1	1197	359	108	32
2	754	226	68	20
3	475	143	43	13
4	299	90	27	8
	30	9	2.7	0.8
	20	6	1.8	0.54
	10	3	0.9	0.27
	5	1.5	0.45	0.135
	3	0.9	0.27	0.08
	1	0.3	0.09	0.027
	0.5	0.15	0.045	0.0135
	0.2	0.06	0.018	0.0054
	0.05	0.015	0.0045	0.00135

Supplementary Table 3. Single channel parameters of the various channels

	P_o			i_{single} (pA)		
Channel	mean	SEM	n	mean	SEM	n
GIRK2	0.088	0.009	38	1.98	0.065	32
IRK1-xFP	0.81	0.028	5	1.38	0.03	7
$GIRK1/2_{HA}$	0.103	0.022	4	2.64	0.081	5
YFP-GIRK1/2 + Gβγ (5 ng RNA)	0.105[1]			2.8[1]		

Supplementary Table 3. Single channel parameters of the various channels involved in the calculation of channel surface density, calibration of YFP in the PM from whole-cell currents of various channels, and in simulations. We used known P_o and i_{single} for YFP-GIRK1/2 and determined P_o and i_{single} experimentally under identical conditions for xFP-IRK1, GIRK2 and $GIRK1/2_{HA}$. The values of P_o and i_{single} are from cell-attached patches, at V_m=-80 mV, in 146 $[K^+]_{out}$. For GIRK2, average i_{single} was derived from patches with P_o>0.05, to avoid filtering effect with short openings.

Supplementary Table 4. Gβ surface density.

What has been measured	mean	SEM	N
Endogenous Gβγ in uninjected oocytes– this study	30	11	4
Endogenous Gβγ in uninjected oocytes – previous study*	24	4	4
Endogenous Gβγ in uninjected oocytes (all data combined)	28	5	8
Endogenous Gβγ in oocytes expressing GIRK2	35	12	3
Expressed Gβγ in oocytes injected with RNAs of GIRK2+**Gβγ****	35	13	3
Expressed Gβγ in oocytes injected with RNAs of GIRK2+ Gβ·$_{YFP}$Gγ **	35	15	3
Expressed Gβγ in oocytes injected with RNAs of GIRK2+ **Gβγ or** Gβ·$_{YFP}$Gγ combined**	35	9	6
Expressed YFP-Gβ in oocytes injected with RNA of YFP-Gβ and WT Gγ*	28	6	4

Supplementary Table 4. Gβ surface density, in μm^{-2}, in naïve oocytes, and surface density of expressed Gβ in oocytes injected with RNAs of Gβ or YFP-Gβ (5 ng) and Gγ (1-2ng) or YFP-Gγ (2-2.5 ng). All surface density measurements were done using the quantitative Western blot (qWB) method.

* Yakubovich et al., 2015[1]

** net expression: Gβγ measured in oocytes expressing GIRK2 alone was subtracted from total Gβ reading.

N is the number of experiments.

Supplementary Table 5. n, N from experiments of Figs. 2 and 4.

Fig. 2h,i	Gβγ coexpressed with:			
	GIRK2: n=		GIRK1/2: n=	
Gβγ RNA (ng)	GMP	Whole oocyte	GMP	Whole oocyte
0.2	25	36	8	22
0.5	27	36	19	32
1	42	36	24	33
2	13	37	5	33
5	47	32	24	32
Number of experiments	N=2 N=3	N=3	N=1 N=2	N=3
Fig. 4a-c	Gβγ coexpressed with:			
	GIRK2: n=		GIRK1/2: n=	
Gβγ RNA (ng)	surface density	whole-cell current	surface density	whole-cell current
0	-	7	-	8
0.2	10	10	12	10
0.5	11	9	6	4
1	10	9	8	5
2	9	5	8	5
5	8	3	8	5
10	10	5	-	-
Number of experiments	N=1 (all data from one experiment)			

For Fig. 4a-c: In this analysis, we included oocytes measured for both YFP-Gγ fluorescence and $I_{\beta\gamma}$, as well as those assessed only for YFP-Gγ expression. 5 ng Gβ was present in all experiments. In the upper table the numbers highlighted in yellow and in cyan correspond to two different sets of experiments.

Supplementary Table 6. The complete fitting results to the WTM model

GIRK2					WTM model, μ=0.3								channel density, μm^{-2}
					Individual cells			Groups			Summary		
Exp. #	method	calibration	GIRK2	See Fig.	c	Kd (μM)	Imax (μA)	c	Kd (μM)	Imax (μA)	Kd (μM)	c	
1	c.a. patch	YFP-GIRK1/2	wt	3	0.037	17.1	Po=0.19				17.3	0.037	(0.91)
2	whole cell	YFP-GIRK1/2	HA					0.044	58.5	8.6	58.4	0.044	12.1
3	whole cell	IRK1-YFP	HA		0	14.7	15.4				14.7	0	21.6
4	whole cell	IRK1-YFP	HA	4a-c	0.039	44.8	25	0.052	45.0	24	44.8	0.039	35.1
5	whole cell	Gβγ from GMPs	wt	Supp. 5				0.010	18.4	17.4	18.4	0.01	12.7
6	whole cell	IRK1-YFP	wt		0.050	34.3	5.63	0.000	23.8	5.1	34.3	0	4.1
				mean	**0.032**	**27.7**	**15.3**	**0.027**	**36.4**	**13.8**	**31.3**	**0.022**	**17.1**
				n	**4**	**4**	**3**	**4**	**4**	**4**	**6**	**6**	**5.0**
				SEM	**0.009**	**6.2**	**4.56**	**0.011**	**8.1**	**3.7**	**6.6**	**0.008**	**5.3**
GIRK1/2					**WTM model, μ=0.3**								
4	whole cell	IRK1-YFP	HA	4a-c	0.250	9.2	16.2	0.24	7.0	14.8	9.2	0.25	
7	whole cell	IRK1-YFP	HA	4d	0.190	1.8	21.5	0.17	5.1	24	1.81	0.19	
8	whole cell	IRK1-YFP	wt		0.350	5.4	12.8	0.31	5.0	13.4	5.4	0.35	
				mean	**0.263**	**5.5**	**16.8**	**0.24**	**5.7**	**17.4**	**5.5**	**0.263**	
				n	**3**	**3**	**3**	**3**	**3**	**3**	**3**	**3**	
				SEM	**0.038**	**1.7**	**2.06**	**0.033**	**0.5**	**2.7**	**1.7**	**0.038**	
$GIRK1_{\Delta dCT}$/GIRK2					**WTM model, μ=0.3**								
7	whole cell	IRK1-YFP	HA	4d	0.097	16.1	39.2	0.06	14.1	38.9	16.125	0.097	
8	whole cell	IRK1-YFP	wt		0.17	20.6	26.1	0.14	21.2	26.3	20.584	0.17	
				mean	**0.134**	**18.4**	**32.6**	**0.1**	**17.7**	**32.6**	**18.355**	**0.134**	
				n	**2**	**2**	**2**	**2**	**2**	**2**	**2**	**2**	
				SEM	**0.026**	**1.6**	**4.64**	**0.028**	**2.5**	**4.5**	**1.6**	**0.026**	

Table S6-continued

GIRK2		WTM model, μ=0.44								Free μ, c=0.03	
		Individual cells			Groups			Summary		Individuals cells	
Exp. #	See Fig.	c	Kd (μM)	Imax (μA)	c	Kd (μM)	Imax (μA)	Kd (μM)	c	μ	Kd (μM)
1	3	0.024	7.4	Po=0.196				7.4	0.024	0.44	7.4
2					0.039	26.4	9.2	26.4	0.039		
3		0	2.7	8.4				2.8	0	fit unstable	
4	4a-c	0.03	18.5	25.6	0.029	12.6	21.4	12.6	0.029	0.62	8.2
5	Supp. 5				0.006	9.6	20	9.6	0.006		
6		0.07	11.2	3.5	0	11.3	5.5	11.2	0.07	fit unstable	
	mean	**0.03**	**10**	**12.5**	**0.019**	**15.0**	**14.05**	**11.3**	**0.028**	**0.53**	**7.8**
	n	**4**	**4**	**3**	**4**	**4**	**4**	**6**	**6**	**2**	**2**
	SEM	**0.013**	**3.1**	**5.5**	**0.008**	**3.3**	**3.42**	**3.1**	**0.009**	**0.06**	**0.3**
GIRK1/2		**WTM model, μ=0.44**									
4	4a-c	0.23	3.3	16.2	0.22	3.1	15.2	3.3	0.23		
7	4d	0.19	0.8	21.9	0.17	2.5	24.9	0.8	0.19		
8		0.34	2.4	13.1	0.31	2.2	13.6	2.4	0.34		
	mean	**0.25**	**2.2**	17.1	**0.23**	**2.6**	**17.9**	**2.2**	**0.25**		
	n	**3**	**3**	**3**	**3**	**3**	**3**	**3**	**3**		
	SEM	**0.04**	**0.6**	**2.1**	**0.03**	**0.2**	**2.9**	**0.6**	**0.04**		
GIRK1$_{\Delta dCT}$/GIRK2		**WTM model, μ=0.44**									
7	4d	0.09	7.5	41.3	0.06	6.6	41.1	7.5	0.09		
8		0.15	8.6	26.5	0.095	8.7	26.9	8.6	0.15		
	mean	**0.12**	**8.0**	**33.9**	**0.078**	**7.6**	**34**	**8.0**	**0.12**		
	n	**2**	**2**	**2**	**2**	**2**	**2**	**2**	**2**		
	SEM	**0.02**	**0.4**	**5.2**	**0.012**	**0.8**	**5**	**0.4**	**0.02**		

Supplementary Table 6. Experimental details and the WTM model fit parameters for all Gβγ dose-dependence experiments. I_{max} is the fitted maximal current. Cooperativity factor μ was fixed at 0.3 or 0.44. Fits with free μ (with fixed c=0.03) were also performed for GIRK2 data, but stable fits were obtained only in two experiments. GIRK2 channel surface density in experiments #2-6 was calculated from I_{max} (fit with μ=0.3) assuming $P_{o,max}$=0.19. In experiment #1 whole-cell currents in the 5 ng Gβ RNA group were 640±136 nA (n=8), corresponding to 0.91 μm^{-2} channel density. All currents in whole-cell mode were recorded in 24 mM $[K]_{out}$ solution. Data are presented for individual cells and groups (where available). In all experiments we measured the surface density of $G\beta\cdot_{YFP}G\gamma$ except #5, where we monitored relative changes in PM-attached Gβ in GMPs (instead of YFP-Gγ) and assumed Gβ density of 40 μm^{-2} with 5 ng Gβ RNA (from Fig. 3). In experiment #2, surface expression of $GIRK2_{HA}$ was measured in groups of cells expressing the different concentration of Gβγ (see Supplementary Methods), and currents were corrected for changes in channel expression.

Supplementary Table 7. p values for pull-down experiments

	p	q	DF
G1NdCT vs. G1NC	0.0001	4.820	51
G1NdCT vs. G1NCΔC1	0.3787	1.913	51
G1NdCT vs. G1NCΔC2	0.0189	3.215	51
G1NdCT vs. G1NCΔC3	0.0134	3.337	51
G1NdCT vs. G1CT	<0.0001	7.222	51
G1NdCT vs. G1(1-40)dCT	<0.0001	6.532	51
G1NdCT vs. G1(40-84)dCT	0.9632	0.9404	51
G1NdCT vs. Sumo dCT	<0.0001	6.853	51
G1NdCT vs. Sumo NT	<0.0001	7.418	51
	p	q	DF
G1NC vs. G1NCΔC1	0.7085	1.389	51
G1NC vs. G1NCΔC2	0.9752	0.8313	51
G1NC vs. G1NCΔC3	0.9998	0.4212	51
G1NC vs. G1CT	0.4784	1.707	51
G1NC vs. G1NdCT	0.0001	4.820	51
G1NC vs. G1(1-40)dCT	0.0932	2.562	51
G1NC vs. G1(40-84)dCT	0.0744	2.659	51
G1NC vs. Sumo dCT	0.1012	2.527	51
G1NC vs. Sumo NT	0.0109	3.389	51

Supplementary Table 7; for Fig. 7: Statistical comparison of Gβγ binding in constructs containing different regions of GIRK1 from pull-down experiments. The table presents p-values (p), t-values (q), and degrees of freedom (DF) for pairwise comparisons using Dunnett's test. G1NC or G1NdCT were used as controls in separate analyses to compare all other samples against them.

Supplementary Table 8. K_d and Hill coefficients from fits to Hill equation for dose-response relations from excised patch measurements.

channel	Gβγ type	preparation	K_d (nM)	n_H	reference
I_{KACh} (GIRK1/4)	$G\beta_1$ or $G\beta_2$ with $G\gamma_2$, $G\gamma_5$ or $G\gamma_7$	atrial myocyte	4-11	1.5	17
GIRK1/3	Bovine brain	*Xenopus* oocyte	11	1.5	22
GIRK 1/4	Bovine brain	*Xenopus* oocyte	10	1.5	
neuronal (GIRK 1/2?)	$G\beta_1\gamma_2$	locus coeruleus neuron	3.78	2.03	23
GIRK1/2	$G\beta_1\gamma_2$	*Xenopus* oocyte	11	1.37-2.04	ref. 9 and Fig. S11
GIRK 1/5 (GIRK5 of *Xenopus*)	$G\beta_1\gamma_2$	*Xenopus* oocyte	1.8-4.75	1.21-1.31	24, 25
I_{KACh} (GIRK1/4)	Bovine brain	atrial myocyte	6	3.12	26

Supplementary Table 9. DNA constructs used in this work

Construct name	Vector	Species	Remarks	Accession number
GIRK1	pGEM-HJ	rat		NP_113798.1
YFP-GIRK1	pGEM-HJ	rat	YFP in NT	
GIRK1Δ123(dCT)	pGEM-HJ	rat	GIRK1 (1-378)	
G1NC WT	pMXT	rat	GIRK1 NT(1-84)-Linker (QSTASQST)-CT(185-501)	
G1NCΔdCT	pMXT	rat	GIRK1 NT(1-84)-Linker (QSTASQST)-CT(184-380)	
G1NdCT	pMXT	rat	GIRK1 NT(1-84)-Linker (QSTASQST)-dCT(381-501)	
G1NCΔC1	pMXT	rat	GIRK1 NT(1-84)-Linker (QSTASQST)-CT(254-501)	
G1NCΔC2	pMXT	rat	GIRK1 NT(1-84)-Linker (QSTASQST)-CT(184-253, 321-501)	
G1NCΔC3	pMXT	rat	GIRK1 NT(1-84)-Linker (QSTASQST)-CT(184-319, 371-501)	
G1N(1-40)dCT	pMXT	rat	GIRK1 NT(1-40)-Linker (QSTASQST)-dCT(381-501)	
G1N(40-84)dCT	pMXT	rat	GIRK1 NT(40-84)-Linker (QSTASQST)-dCT(381-501)	
Sumo-G1NT	pGEM-HJ	rat	Sumo-GIRK1 NT(1-84)	
G1CT	pMXT	rat	GIRK1 CT(184-501)	
Sumo-G1dCT	pMXT	rat	Sumo-GIRK1 dCT(381-501)	
GIRK2	pGEM-HJ	mouse	GIRK2A, 414 a.a.	NP_001020755.1
G2NC	PGBXW	mouse	GIRK2 NT(1-95) Linker (QSTASQST) CT(194-414)	
$GIRK2_{trunc}$	pGEM-HJ	mouse	52-380 a.a	
$G2NC_{trunc}$	pGEM-HJ	mouse	GIRK2 NT(52-95) Linker (QSTASQST) CT(194-380)	
GIRK2-HA	pGEM-HJ	mouse	HA tag in P-loop --MDHI-HA-EDPS--	
GIRK2-CFP	pGEM-HJ	mouse	CFP in CT	
M2R	pGES	human		NP_001006631.1
IRK1-YFP, IRK1-CFP	pGSB	mouse	YFP or CFP in CT	NP_032451.1
Gβ1 wt	pGEM-HE	bovine		NP_786971.2
Myr-Gβ1	pGEM-HJ	bovine	myristoylated Gβ1	
Supplementary Table 9 continued				
YFP-Gβ1	pGEM-HJ	Bovine	YFP in NT with a Lys-Ser linker	
Split Venus2-Gβ1	pGEM-HJ	human	Split Venus2 in NT	
Gβ1-6Gly-YFP	pGEM-HJ	bovine	YFP in CT, fused to Gβ1 by a linker of GGGGGG (6 glycines)	

CFP-2Gly-Gβ1	pGEM-HJ	bovine	YFP in NT, fused to Gβ by a linker of GG (2 glycines)	
Gγ2	pGEM-HJ	bovine		P63212.2
Gγ2 C68S	pGEM-HE	bovine		
Split Venus1-Gγ2	pGEM-HJ	bovine	Split Venus1 in NT	
YFP-Gγ2	pMXT	bovine	YFP in NT	
$G\alpha_{i3}$	pGEM-HJ	human		NP_006487.1
Phosducin	pGEM-HE	bovine	myristoylated phosducin	NP_002588.3

Mouse GIRK2 (GIRK2A, 414 a.a.), $GIRK2_{HA}$, C-terminally CFP labeled GIRK2 (GIRK2-CFP), bovine $G\beta_1$, bovine $G\gamma_2$, human m2R, rat GIRK1, N-terminally YFP labeled GIRK1 (YFP-GIRK1), N-terminally YFP labeled $G\gamma_2$ (YFP-$G\gamma_2$), N-terminally YFP labeled $G\beta_1$ (YFP-Gβ, with a Lys-Ser linker), G1NC (the cytosolic N-a.a. 1-84 and C-termini a.a 183-501 of GIRK1 connected by an 8-a.a. linker, QSTASQST), G2NC (the full cytosolic N- a.a. 1-95 and C-termini a.a. 194-404 of GIRK2 connected by a 2-a.a. linker, Lys-Leu), full length human $G\alpha_{i3}$ and myristoylated bovine phosducin were described previously[8, 27-29]. TEVC, two-electrode whole-cell voltage clamp.

Supplementary Table 10. Antibodies used in this study

Antibody	SOURCE	IDENTIFIER
Donkey IgG	Jackson ImmunoResearch Labs	Cat. No. 017-000-003; RRID:AB_2337256; Lot 131795
Rabbit polyclonal anti-Gβ (T-20)	Santa Cruz Biotechnology	Cat. No. sc-378; RRID:AB_631542; currently discontinued
GNB1	GeneTex	GTX114442; RRID:AB_10619473; Lot 43565
Goat Anti-Rabbit IgG H&L–DyLight650	Abcam	ab96886; RRID:AB_10680254; Lot GR3228258-6
Anti-His_6 Peroxidase mouse monoclonal, clone BMG-His-1	Roche	Cat. No. 11 965 085 001; RRID: AB_514487
Goat Anti-Rabbit IgG, (H+L) HRP conjugated	Jackson ImmunoResearch Labs	Cat. No. 111-035-144, RRID:AB_2307391

Supplementary references

1. Yakubovich D*, et al.* A quantitative model of the GIRK1/2 channel reveals that its basal and evoked activities are controlled by unequal stoichiometry of Gα and Gβγ. *PLoS Comput Biol* **11**, e1004598 (2015).

2. Berlin S*, et al.* A collision coupling model governs the activation of neuronal GIRK1/2 channels by muscarinic-2 receptors. *Front Pharmacol* **11**, 1216 (2020).

3. Dascal N, Kahanovitch U. The roles of Gβγ and Gα in gating and regulation of GIRK channels. *Int Rev Neurobiol* **123**, 27-85 (2015).

4. Ivanova-Nikolova TT, Nikolov EN, Hansen C, Robishaw JD. Muscarinic K^+ channel in the heart. Modal regulation by G protein βγ subunits. *J Gen Physiol* **112**, 199-210 (1998).

5. Sadja R, Alagem N, Reuveny E. Graded contribution of the Gβγ binding domains to GIRK channel activation. *Proc Natl Acad Sci U S A* **99**, 10783-10788 (2002).

6. Touhara KK, MacKinnon R. Molecular basis of signaling specificity between GIRK channels and GPCRs. *Elife* **7**, (2018).

7. Sarvazyan NA, Remmers AE, Neubig RR. Determinants of G_{i1}α and βγ binding. Measuring high affinity interactions in a lipid environment using flow cytometry. *J Biol Chem* **273**, 7934-7940 (1998).

8. Kahanovitch U*, et al.* Recruitment of Gβγ controls the basal activity of G-protein coupled inwardly rectifying potassium (GIRK) channels: crucial role of distal C terminus of GIRK1. *J Physiol* **592**, 5373-5390 (2014).

9. Peleg S, Varon D, Ivanina T, Dessauer CW, Dascal N. Ga_i controls the gating of the G-protein-activated K^+ channel, GIRK. *Neuron* **33**, 87-99 (2002).

10. Sarvazyan NA, Lim WK, Neubig RR. Fluorescence analysis of receptor-G protein interactions in cell membranes. *Biochemistry* **41**, 12858-12867 (2002).

11. Sawai T, Hirakawa T, Yamada K, Nishizawa Y. Interaction between Pleckstrin homology domains and G protein βγ subunits: analyses of kinetic parameters by a biosensor-based method. *Biol Pharm Bull* **22**, 229-233 (1999).

12. Zheng S, Abreu N, Levitz J, Kruse AC. Structural basis for KCTD-mediated rapid desensitization of GABAB signalling. *Nature* **567**, 127-131 (2019).

13. De Waard M, Liu H, Walker D, Scott VE, Gurnett CA, Campbell KP. Direct binding of G-protein βγ complex to voltage-dependent calcium channels. *Nature* **385**, 446-450 (1997).

14. Savage JR, McLaughlin JN, Skiba NP, Hamm HE, Willardson BM. Functional roles of the two domains of phosducin and phosducin-like protein. *J Biol Chem* **275**, 30399-30407 (2000).

15. Carman CV*, et al.* Mutational analysis of Gbg and phospholipid interaction with G protein-coupled receptor kinase 2. *J Biol Chem* **275**, 10443-10452 (2000).

16. Runnels LW, Scarlata SF. Determination of the affinities between heterotrimeric G protein subunits and their phospholipase C-β effectors. *Biochemistry* **38**, 1488-1496 (1999).

17. Krapivinsky G, Krapivinsky L, Wickman K, Clapham DE. Gbg binds directly to the G protein-gated K^+ channel, I_{KACh}. *J Biol Chem* **270**, 29059-29062 (1995).

18. Krapivinsky G, Kennedy ME, Nemec J, Medina I, Krapivinsky L, Clapham DE. Gβ binding to GIRK4 subunit is critical for G protein-gated K^+ channel activation. *J Biol Chem* **273**, 16946-16952 (1998).

19. Doupnik CA, Dessauer CW, Slepak VZ, Gilman AG, Davidson N, Lester HA. Time resolved kinetics of direct Gb_1g_2 interactions with the carboxyl terminus of Kir3.4 inward rectifier K^+ channel subunits. *Neuropharmacol* **35**, 923-931 (1996).

20. Yokogawa M, Osawa M, Takeuchi K, Mase Y, Shimada I. NMR analyses of the Gβγ binding and conformational rearrangements of the cytoplasmic pore of G protein-activated inwardly rectifying potassium channel 1 (GIRK1). *J Biol Chem* **286**, 2215-2223 (2011).

21. Wang W, Touhara KK, Weir K, Bean BP, MacKinnon R. Cooperative regulation by G proteins and Na^+ of neuronal GIRK2 K^+ channels. *Elife* **5**, (2016).

22. Jelacic TM, Sims SM, Clapham DE. Functional expression and characterization of G-protein-gated inwardly rectifying K+ channels containing GIRK3. *J Membr Biol* **169**, 123-129 (1999).

23. Albsoul-Younes AM*, et al.* Interaction sites of the G protein β subunit with brain G protein-coupled inward rectifier K^+ channel. *J Biol Chem* **276**, 12712-12717 (2001).

24. Luchian T*, et al.* A C-terminal peptide of the GIRK1 subunit directly blocks the G protein-activated K^+ channel (GIRK) expressed in *Xenopus* oocytes. *J Physiol* **505 (Pt 1)**, 13-22 (1997).

25. Schreibmayer W*, et al.* Inhibition of an inwardly rectifying K channel by G-protein α-subunits. *Nature* **380**, 624-627 (1996).

26. Ito H*, et al.* On the mechanism of G protein βγ subunit activation of the muscarinic K^+ channel in guinea pig atrial cell membrane. Comparison with the ATP-sensitive K^+ channel. *J Gen Physiol* **99**, 961-983 (1992).

27. Rishal I, Porozov Y, Yakubovich D, Varon D, Dascal N. Gβγ-dependent and Gβγ-independent basal activity of G protein-activated K^+ channels. *J Biol Chem* **280**, 16685-16694 (2005).

28. Rubinstein M*, et al.* Divergent regulation of GIRK1 and GIRK2 subunits of the neuronal G protein gated K^+ channel by Ga_iGDP and Gbg. *J Physiol* **587**, 3473-3491 (2009).

29. Berlin S*, et al.* Two distinct aspects of coupling between Gαi protein and G protein-activated K^+ channel (GIRK) revealed by fluorescently labeled $G\alpha_{i3}$ protein subunits. *J Biol Chem* **286**, 33223-33235 (2011).